Chem. Senses 30: 69–80, 2005 doi:10.1093/chemse/bji002

Comparison of Odorant Specificity of Two Human Olfactory Receptors from Different Phylogenetic Classes and Evidence for Antagonism

Guenhaël Sanz, Claire Schlegel, Jean-Claude Pernollet and Loïc Briand

Biochimie de l'Olfaction et de la Gustation, Neurobiologie de l'Olfaction et de la Prise Alimentaire, INRA, Domaine de Vilvert, Bâtiment 526, F 78352 Jouy-en-Josas Cedex, France

Correspondence to be sent to: Jean-Claude Pernollet, Biochimie de l'Olfaction et de la Gustation, Neurobiologie de l'Olfaction et de la Prise Alimentaire, INRA, Domaine de Vilvert, Bâtiment 526, F 78352 Jouy-en-Josas Cedex, France. e-mail : Jean.Claude.Pernollet@jouy.inra.fr

Abstract

Humans are able to detect and discriminate myriads of odorants using only several hundred olfactory receptors (ORs) classified in two major phylogenetic classes representing ORs from aquatic (class I) and terrestrial animals (class II). Olfactory perception results in a combinatorial code, in which one OR recognizes multiple odorants and different odorants are recognized by different combinations of ORs. Moreover, recent data suggest that odorants could also behave as antagonists for other ORs, thus making the combinatorial coding more complex. Here we describe the odorant repertoires of two human ORs belonging to class I and class II, respectively. For this purpose, we set up an assay based on calcium imaging in which 100 odorants were screened using air-phase odorant stimulation at physiological doses. We showed that the human class I OR52D1 is functional, exhibiting a narrow repertoire related to that of its orthologous murine OR, demonstrating than this human class I OR is not an evolutionary relic. The class II OR1G1 was revealed to be broadly tuned towards odorants of 9–10 carbon chain length, with diverse functional groups. The existence of antagonist odorants for the class II OR was also demonstrated. They are structurally related to the agonists, with shorter carbon chain length.

Key words: agonist, calcium imaging, inhibition, olfaction

Introduction

All living organisms, including human beings, are able to detect and discriminate myriads of structurally diverse odorants. This chemosensory function is mediated by olfactory receptors (ORs) embedded in the plasma membrane of the olfactory neurons located in the olfactory epithelium. It is generally accepted that perception of odorant quality results in a combinatorial code, in which one OR recognizes multiple odorants and different odorants are recognized by different combinations of ORs (Duchamp-Viret *et al.*, 1999; Malnic *et al.*, 1999). However, recent data have revealed an additional aspect in receptor coding for the perception of odorant mixtures demonstrating that odorants could act both as agonist for some ORs and as antagonist for others (Duchamp-Viret *et al.*, 2003; Araneda *et al.*, 2004; Oka *et al.*, 2004). This dual agonist/antagonist combinatorial coding is in good agreement with behavioral and psychophysical observations of mixture perception, designated as odor masking or counteraction phenomenon (Laing and Francis, 1989; Cometto-Muniz *et al.*, 1999).

ORs belong to the G-protein coupled receptors family and are encoded by an exceptionally large multigene family. Analysis of the human genome draft sequences has revealed ~650 human OR genes with 350 potentially functional genes (Glusman *et al.*, 2001; Zozulya *et al.*, 2001; Malnic *et al.*, 2004). The human OR genes, like those of other mammals, were classified according to class I (fish-like) ORs, originally identified in fish (Ngai *et al.*, 1993), and class II (terrestrial-type) ORs, subsequently found in vertebrate species to be intermixed with class I ORs (Freitag *et al.*, 1995). Class I ORs were initially suggested to be evolutionary relics in humans (Buettner *et al.*, 1998; Bulger *et al.*, 1999). However, the pseudogene fraction among the human class I ORs (52%), considerably lower than that observed for human class II ORs (77%) (Glusman *et al.*, 2001), strengthens the idea than human class I receptors could be functional.

Due to the difficulty to functionally express ORs in heterologous cells, identification of OR repertoires have been obtained for only a few rodent ORs, all belonging to class II (Krautwurst *et al.*, 1998; Touhara *et al.*, 1999; Gaillard *et al.*, 2002, 2004; Oka *et al.*, 2004). Only one narrowly tuned human class II (OR17-40) has been shown to recognize helional and other close structurally related odorants

(Wetzel *et al.*, 1999). To our knowledge, no functional data are yet available on human class I ORs. However, using a combination of calcium imaging and single-cell reverse transcriptase-polymerase chain reaction (RT-PCR), Malnic and colleagues have shown that mouse olfactory neurons expressing class I ORs were capable of responding to aliphatic alcohols and carboxylic acids (Malnic *et al.*, 1999).

In the present work, we set up a new method of odorant application called volatile-odorant funtional assay (VOFA), which permits to stimulate cells with odorant as vapor phase (Figure 1A). This mode of odorant delivery permits (i) the avoidance of tubing that can be irreversibly contaminated by applying sticky odorants to the bath; ii) the avoidance of mechanical disturbances of the cells that may occur during a perfusion of the bath chamber, which may lead to signal artifacts; iii) the avoidance of problems of laminar flow in the bath chamber often designed rather simple; and (iv) the study of the functional role of odorant-binding protein as an odorant carrier to ORs. However, VOFA presents also major disadvantages: (i) cell stimulation is not synchronized forbiding a simple averaging of the signals of single cells; (ii) the amount of odorant corresponding to the physiological range and reaching cells cannot be known; and (iii) desensitization experiments and wash-out of odorants is not possible.

Using VOFA, we established the odorant repertoire of two human ORs. The class I OR52D1 was chosen because it is the ortholog of the known mouse OR S19 (Genbank accession number AF121976), for which some ligands have been described (Malnic *et al.*, 1999), whereas the class II OR1G1 was studied because it has been proved to be expressed in nasal epithelium (Matarazzo *et al.*, 2002). We compared OR52D1 and OR1G1 repertoires and identified antagonists for OR1G1.

Materials and methods

Materials and reagents

Odorants were purchased from Sigma-Aldrich, Fluka or Acros Organics (Noisy-le-Grand, France) at the highest purity available. Odorant solutions were prepared as 100 mM stocks in 100% MeOH (Spectroscopic grade; Sigma) and stored at −20°C. Individual odorants and mixtures were made up fresh by dilutions of stock solutions to the final working solution in 100% MeOH. ATP was purchased from Sigma.

Vector constructions

For construction of a selectable plasmid expressing $G_{\alpha 16}$ protein subunit, $G_{\alpha 16}$ cDNA (kindly provided by D. Krautwurst, German Institute of Human Nutrition, Bergholz-Rehbrücke, Germany) was amplified by PCR using the following specific primers: 5′-GCGGGCAAGCTTATGGCCCGCTCGCTGACC-3′ and 5′-GCGCGCCTCGAGTCACAGCAGGTTGATCTC-3′, and subcloned between the restriction sites *Hin*dIII and *Xho*I of pcDNA3.1/Hygro(+) mammalian expression vector (Invitrogen) generating the pcDNA3.1/HygroG16 plasmid. In order to help ORs to translocate to the plasma membrane, we used a chimeric OR expression construct engineered with a rhodopsin amino-terminal extension. A PCR fragment containing the first 108 nucleotides of the coding region of bovine rhodopsin [amplified by PCR from YOPS-PHIL-S1 vector (Abdulaev *et al.*, 1997), kindly provided by K.D. Ridge, Center for Advanced Research in Biotechnology, Rockville, MD] was digested by *Bam*HI and *Pst*I and introduced into mammalian expression vector pCMV-Tag3 (Stratagene, Saint-Quentin-en-Yvelines, France). The resulting vector (pCMV-RhoTag) was used as a cassette to introduce OR genes. Rat rIC6 gene was amplified by PCR from rat genomic DNA (Novagen, Fontenay-sous-Bois, France) using specific primers designed from mouse mIC6 sequence (Krautwurst *et al.*, 1998): 5′-CCAGGAGAATTCGCGAACAGCACTACTGTTACTGAGTTTATTTTGCTGGGG-3′ and 5′-CCCGGGGAGCTCAGTGCAGACCGACTTGAAAACCTTGAACGA-3′. OR52D1 and OR1G1 genes [Human Olfactory Receptor Data Exploratorium (HORDE) classification, Genbank accession numbers BD144374 and AX377081, respectively] were amplified by PCR from human genomic DNA (Novagen, Fontenay-sous-Bois, France) using the OR52D1 specific primers (5′-CCAGGAGAATTCTCAGATTCCAACCTCAGTGATAACCATCTTCCAGACACC-3′ and 5′-CCCCTCGAGTCATATTGAAGTCTTCCCCAGGTGAAGCAGTTT-3′) and OR1G1 specific primers (5′-CCAGGAGAATTCGAGGGGAAAAATCTGACCAGCATCTCAGAATGTTTCCTC-3′ and 5′-GGGCCCCTCGAGCTAAGGGGAATGAATTTTCCGAACCCA-3′). The PCR fragments were subsequently cloned into pCMV-RhoTag using *Eco*RI and *Xho*I restriction sites. The resulting vectors (pCMV-RhoTagrIC6, pCMV-RhoTagOR1G1 and pCMV-RhoTagOR52D1) encode the 10-amino acid c-myc epitope in frame with the first 36 amino acids of bovine rhodopsin joined to the full-length cDNAs of rIC6, OR52D1 and OR1G1. The β_2-adrenergic receptor (β_2-AR) was subcloned into pCMV-Tag3 vector generating the pCMV-Tagβ2 plasmid.

Cell culture and transfection of HEK293 cells

HEK293 cells (Human Embryo Kidney cells) and HEK293 derivatives that stably express $G_{\alpha 16}$ and/or ORs were cultured in Minimum Essential Medium (GIBCO, Invitrogen Corporation, Cergy-Pontoise, France) supplemented with 10% fetal bovine serum (Eurobio, Les Ulis, France), 2 mM L-glutamine (GIBCO, Cergy-Pontoise, France) and Eagle's non-essential amino acids (Eurobio, Les Ulis, France) at 37°C in a humidified incubator with 5% CO_2. HEK293 cells were stably transfected with pcDNA3.1/HygroG16 plasmid using Lipofectamine™ 2000 (Invitrogen Life Technologies, Cergy-Pontoise, France) according to the manufacturer

instructions. Forty-eight hours after transfection, $G_{\alpha 16}$-expressing HEK293 cells were selected by treatment with 300 μg/mL hygromycin B (Sigma). rIC6-, OR1G1- and OR52D1-expressing stable cell lines were generated by transfecting pCMV-RhoTagrIC6, pCMV-RhoTagOR1G1 and pCMV-RhoTagOR52D1 vectors into HEK293 cells or $G_{\alpha 16}$-expressing HEK293 cells. Stable cells expressing ORs were selected with 1 mg/ml neomycin (Sigma) and frozen in several cryovials in order to use the same cell batches over the study. All cells used were <10 passages.

Confocal immunofluorescence microscopy

Twenty-four hours after transfection, cells transiently transfected with pCMV-Tagβ2, pCMV-RhoTagrIC6, pCMV-RhoTagOR1G1 and pCMV-RhoTagOR52D1 were plated on poly-L-lysine-coated 96-well tissue-culture plate (μClear, Greiner Bio-one, Poitiers, France). After an additional 24 h, living cells were rinsed twice with calcium assay buffer [Hanks' salt solution (Eurobio, Les Ulis, France) supplemented with 20 mM HEPES, pH 7.2] and incubated with monoclonal anti-c-myc–Cy3 conjugate antibody (Sigma) for 1 h at room temperature at 1:100 dilution in calcium assay buffer. Cells were washed three times with calcium assay buffer and scanned with a Zeiss LSM 510 laser scanning confocal microscope.

Calcium imaging

HEK293 derivative cells were seeded onto a poly-L-lysine-coated 96-well tissue culture plate (μClear, Greiner Bio-one, Poitiers, France), at a density of 1×10^5 cells per well. Twenty-four hours post-seeding, cells were washed once with calcium assay buffer. Cells were loaded 30 min at 37°C with 2.5 μM of the Ca^{2+}-sensitive fluorescent dye Fluo-4 acetoxymethyl ester (Molecular Probes, Leiden, The Netherlands), prepared in calcium assay buffer supplemented with 0.025% (w/v) pluronic acid (F-127, Molecular Probes, Leiden, The Netherlands) and 0.1% (w/v) bovine serum albumin. Cells were washed twice with calcium assay buffer and the resulting volume of assay buffer covering cells was 60 μl. Cells were then incubated for 10 min at 37°C in the incubator and 10 min in the dark at 28°C. Calcium imaging was carried out at room temperature using an inverted epifluorescence microscope (CK40 Olympus, Rungis, France) equipped with a digital camera (ORCA-ER, Hamamatsu Photonics, Massy, France). Ca^{2+} reponses were recorded under ×10 magnification at 485 nm excitation and 510 nm emission wavelengths. Images were taken every second during 10 min using a bining ×4. The SimplePCI software (Hamamatsu, Compix, Massy, France) was used for data acquisition and analysis. The Ca^{2+} signal was expressed as fractional change in fluorescence light intensity: $\Delta F/F = (F - F_0)/F_0$, where F is the fluorescence light intensity at each point and F_0 is the value of emitted fluorescent light before the stimulus application. Increased receptor activity in $G_{\alpha 15/16}$-based assays is reflected not only in increased magnitude of the calcium responses of individual cells but also in increased number of responding cells (Li *et al.*, 2002). Therefore, we quantitated OR activity by counting the number of responding cells. Cells were counted as responders when $\Delta F/F$ change was at least twice the baseline $\Delta F/F$ fluctuation. For data analysis, Ca^{2+} cell response refers to the percentage of responding cells normalized to those responding to the application of 100 μM ATP in a field of ~400 cells. ATP was applied at the end of each experiment with a micropipette at 100 μM. ATP was used as a control for the ability of cells to produce calcium responses because it stimulates HEK intrinsic purinergic receptors coupled to the inositol 1,4,5-triphosphate (IP3) pathway via endogenous G proteins. Isoproterenol (10 μM) was manually applied like ATP and used as a control for $G_{\alpha 16}$-expressing cells because it stimulates HEK293 endogenous β_2-adrenergic receptors. The Ca^{2+} response induced by isoproterenol in HEK cells is dependent on cotransfection with the $G_{\alpha 16}$ subunit (Krautwurst *et al.*, 1998). We observed that the number of $G_{\alpha 16}$-expressing cells responding to isoproterenol was ~90% of cells responding to ATP. Odorants were tested at concentrations that do not elicit calcium responses from mock-transfected $G_{\alpha 16}$-expressing cells. Since cells were not clonally derived and OR or $G_{\alpha 16}$ expression could vary over time, we also controlled that the number of responding cells to a given odorant was constant over ten cell passages. All experiments were made at least twice to ensure result validity.

Agonist and antagonist screening using volatile-odorant functional assay (VOFA)

Agonist and antagonist screening was achieved using VOFA, which permits to stimulate cells with odorant as vapor phase (Figure 1A). Experiments were conducted with cells seeded in 96-well tissue-culture plate covered with 60 μl of calcium assay buffer, corresponding to a 1.5 mm height of liquid in the wells. Plate was sealed with a transparent adhesive plastic film (Viewseal, Greiner Bio-one, Poitiers, France). Odorants were diluted into 100% MeOH, at concentrations ranging from 0.01 to 100 μM. The plastic film was pierced using a syringe needle. Using a 10 μl Hamilton syringe, a 1 μl drop of MeOH diluted odorant was introduced in the sealed well and hanged beneath the inner face of the plastic film. The tiny hole was then filled up using vacuum grease and calcium imaging started. The MeOH drop evaporated freely in a few seconds, leading to a progressive stimulation of cells. ATP was applied at the end of each experiment at 100 μM to ensure cell viability. When antagonist odorants were screened, agonist and antagonist were mixed into MeOH and co-applied as a 1 μl drop.

Results

Set up of the VOFA

Calcium imaging of transfected mammalian cells was shown to be an efficient method to study functionally expressed ORs

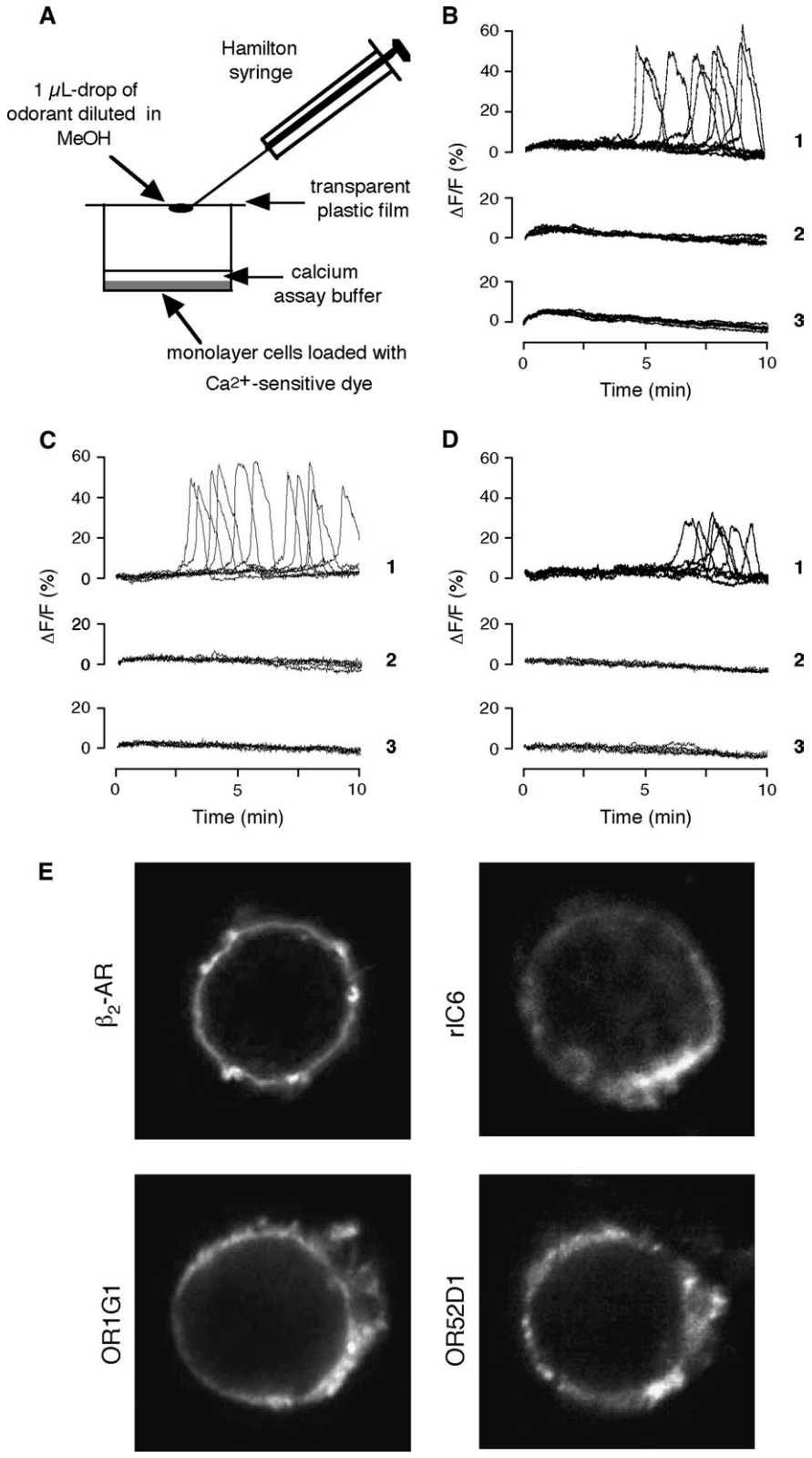

Figure 1 Introduction to the assay and OR responses. **(A)** Schematic drawing of the VOFA used for odorant stimulation. Cell seeded in a 96-well tissue culture plate were loaded with Ca^{2+}-sensitive dye and covered with 60 μl of calcium assay buffer. Wells were sealed with a transparent adhesive plastic film. MeOH diluted odorant was applied using a 10 μl Hamilton syringe as a 1 μl drop hanging beneath the inner face of the plastic film. The MeOH drop evaporated freely in a few seconds, leading to progressive stimulation of cells with odorant as vapor phase. **(B)** Odorant-induced Ca^{2+} responses of rIC6 using VOFA. HEK293 cells

(Krautwurst *et al.*, 1998; Touhara *et al.*, 1999; Wetzel *et al.*, 1999; Kajiya *et al.*, 2001; Gaillard *et al.*, 2002, 2004; Oka *et al.*, 2004). Because some odorants were recently shown to act as OR antagonists (Araneda *et al.*, 2000; Spehr *et al.*, 2003; Oka *et al.*, 2004), we aimed at testing OR activation using single odorants, avoiding mixtures. In contrast to previously published studies (Krautwurst *et al.*, 1998; Gaillard *et al.*, 2002, 2004; Katada *et al.*, 2003; Oka *et al.*, 2004) in which odorants were applied as solutions perfused onto cultured cells, we designed a volatile-odorant functional assay (VOFA). This assay allows delivering odorants as vapor phase (Figure 1A).

We set up the system with rIC6, a rat OR orthologous to the murine OR mIC6 (sharing 95% amino-acid sequence identity). mIC6 is known to be activated by (−)-citronellal in HEK293 cells co-transfected with the promiscuous G protein, $G_{\alpha 16}$, which couples the receptor to an IP3-mediated signalling cascade leading to an increase in intracellular calcium level (Krautwurst *et al.*, 1998). Using rIC6/$G_{\alpha 16}$-stably expressing HEK293 cells, we revealed OR activation using Fluo-4 as calcium sensitive fluorescent probe. (−)-Citronellal was applied diluted in a 1 µl MeOH drop, at a concentration of 100 µM. The hanging drop freely evaporated in a few seconds, leading to a progressive stimulation of up to 20% of cells, measured during a 10 min recording period. Observation of time-course activation of single rIC6/$G_{\alpha 16}$-expressing cells stimulated with (−)-citronellal showed asynchronous Ca^{2+} activations after a lag-phase of several minutes (Figure 1B-1). As control, MeOH without odorant was unreactive on rIC6/$G_{\alpha 16}$-expressing HEK293 cells (Figure 1B-2). Moreover, no Ca^{2+} response was observed when (−)-citronellal was applied on $G_{\alpha 16}$-expressing cells, even at 1 mM concentration in a 1 µl drop (Figure 1B-3). Localization of rIC6 at the plasma membrane was demonstrated by immunofluorescence staining with anti-c-myc antibody (raised against N-terminal extracellular myc epitope) on non-permeabilized cells transiently transfected, with β_2-adrenergic receptor as the control. The immunofluorescence signal was clearly observed for both receptors at the plasma membrane, delimiting a typical ring of labeling around the cell surface (Figure 1E).

Similar results were observed with both studied human ORs (Figure 1C–E). The class I receptor OR52D1 and class II receptor OR1G1, cloned from human genomic DNA, modified with the rhodopsin N-terminal end, were independently used to create stable cell lines co-expressing $G_{\alpha 16}$-protein. Stimulation of both cell lines with odorants elicited an increase in intracellular Ca^{2+} level. As shown in Figure 1C-1,D-1, OR1G1/$G_{\alpha 16}$- and OR52D1/$G_{\alpha 16}$-expressing cells responded to a 1 µl drop of 10 µM nonanal and 10 µM methyl octanoate, respectively. Control cell lines, deprived of OR gene, but expressing $G_{\alpha 16}$ protein, were not responsive to either odorant (Figure 1C-2,D-2). We also tested whether OR responses were dependent on co-expression of $G_{\alpha 16}$-protein. For both ORs, no Ca^{2+} response was observed in absence of $G_{\alpha 16}$, demonstrating that $G_{\alpha 16}$ protein is essential to couple ORs to the IP3 pathway in HEK293 cells (Figure 1C-3,D-3). To determine whether odorant-induced Ca^{2+} cell responses were dose dependent, we stimulated OR1G1/$G_{\alpha 16}$-expressing cells with nonanal diluted in a 1 µl MeOH drop, at concentrations ranging from 0.01 to 100 µM (Figure 2A). As shown by Li *et al.* (2002), we observed that increased ligand concentration resulted not only in increased magnitude of the calcium responses of individual cells but also in increased numbers of responding cells (Figure 2B,C). Therefore, we quantitated OR activity by counting the number of responding cells. We also verified that the number of responding cells to a given odorant did not vary significantly over 10 cell passages. As soon as a strong ligand was identified for each OR studied (nonanal and methyl octanoate for OR1G1 and OR52D1, respectively), all other odorants were tested using these odorants as positive controls. Before testing odorant molecules, we verified that control cell lines, deprived of OR gene but expressing $G_{\alpha 16}$ protein, were not responsive to odorants at concentrations ranging from 10 µM to 1 mM in a 1 µl drop. Ninety-five compounds among 103 chemicals tested did not elicit Ca^{2+} response in these control cells and were used in this study, while eight (citronellol, linalool, 2-phenyl ethanol, eugenol, dimetol, α-pinene, lilial and 2,4-dithiopentane) were excluded because they induced non-specific Ca^{2+} responses (data not shown). Considering that high odorant concentration in the drop (>1 mM for most odorants, and >100 µM for others) also induced non-specific Ca^{2+} responses, cells were stimulated with 10 µM odorant concentration in a 1 µl drop.

Identification of odorants activating OR1G1, a class II human receptor

Odorants were tested individually to avoid any inhibitory effect on OR1G1/$G_{\alpha 16}$-expressing cells at a concentration of 10 µM in a 1 µl drop. We found that various odorants belonging

co-expressing rIC6 and $G_{\alpha 16}$ were stimulated with a 1 µl drop of 100 µM (-) citronellal (1) or MeOH alone (2). Ca^{2+} responses were recorded during 10 min and are shown as fluorescence intensity changes (ΔF/F). As a control, $G_{\alpha 16}$ expressing HEK293 cells without OR were stimulated with 1 µl drop of 1 mM (-) citronellal (3). At the end of each experiment, ATP (100 µM) was applied to verify cell viability. The curves are representative Ca^{2+} responses of nine responsive single cells out of 81 within the same camera field. **(C)** Representative Ca^{2+} response profiles of cells expressing OR1G1 and $G_{\alpha 16}$ (1), $G_{\alpha 16}$ alone (2) and OR1G1 alone (3) stimulated with a 1 µl drop of 10 µM nonanal. **(D)** Representative Ca^{2+} response profile of cells expressing OR52D1 and $G_{\alpha 16}$ (1), $G_{\alpha 16}$ alone (2) and OR52D1 alone (3) stimulated with a 1 µl drop of 10 µM methyl octanoate. At the end of each experiment, ATP (100 µM) was applied to verify cell viability. Data are shown as fluorescence intensity changes (Δ*F*/*F*). The curves are representative Ca^{2+} responses of 7–11 responsive HEK293 cells within the same camera field. **(E)** Confocal microscopic images of non-permeabilized HEK293 cells transiently expressing β_2-AR, rIC6, OR1G1 and OR52D1. Receptors were visualized at the plasma membrane by immunofluorescence using anti-c-myc antibody.

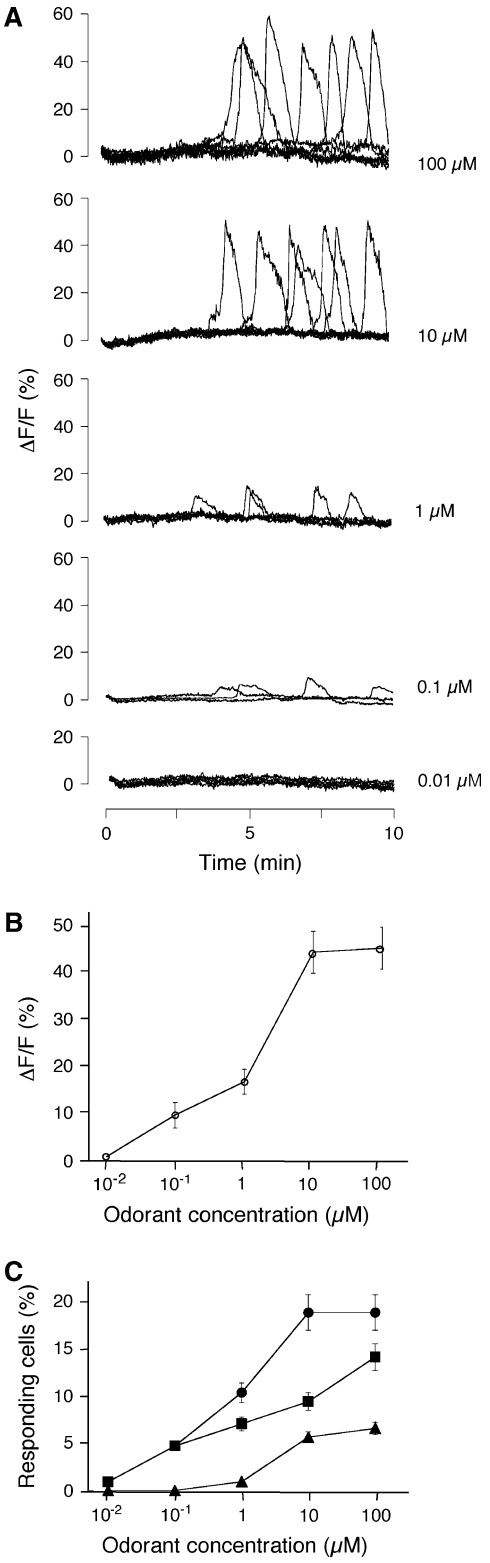

Figure 2 Dose responses for OR1G1. **(A)** HEK293 cells co-expressing $G_{\alpha 16}$ and OR1G1 were stimulated with nonanal at concentrations of 0.01, 0.1, 1, 10 and 100 μM in 1 μl drop. Data are shown as fluorescence intensity changes ($\Delta F/F$). The curves are representative Ca^{2+} responses of 4–7 responsive HEK293 cells within the same camera field. **(B)** Dose–response curve of OR1G1 for nonanal. The data are shown as the average of Ca^{2+} response magnitudes of the responding cells recorded during 10 min. Bars indicate standard deviation (three independent experiments). **(C)** Dose–response curves of OR1G1 for nonanal (circles), decanoic acid (squares) and 1-hexanol (triangles). Ca^{2+} responses were recorded during 10 min. Data are shown as the number of responding cells normalized as percentage of cells responding to 100 μM ATP. Bars indicate standard deviation (three independent experiments).

to different chemical classes differently elicited OR1G1 Ca^{2+} responses. We classified odorants according to the percentage of responding cells: strong agonists elicited a response in >15% of cells, medium agonists 10–15% of cells, and weak agonists 5–10% of cells. Finally, because $G_{\alpha 16}$-expressing cells showed nonspecific Ca^{2+} responses ranging from 1 to 2% of cells, odorants eliciting <5% of cells were considered as non-agonist. As illustrated in Figure 3, most active odorants (i.e. strong and medium agonists) are 8-, 9- and 10-carbon molecules, with an optimum for 9-carbon length. As regards chemical functions, among the five strong agonists which exhibited aliphatic chains, we found two alcohols (2-ethyl-1-hexanol, 1-nonanol), one ester (ethyl isobutyrate), one lactone (γ-decalactone) and one aldehyde (nonanal). Among medium agonists, we also observed thioesters, ketones, one aliphatic acid, and diverse cyclic molecules such as pyrazines and thiazols. It is worth emphasizing that aliphatic molecules with a same function exhibited a critical size, 9 carbons for aldehydes, ketones and alcohols, and 10 carbons for aliphatic acids. In contrast to aliphatic compounds, some cyclic molecules with 11 or more carbons were observed as medium agonists (trans-anethol, piperonyl acetone, lyral and hedione). The position of the functional group in aliphatic molecules was not essential for OR1G1 elicitation, except for 9-carbon alcohols since 1-nonanol was far more active than 2-nonanol.

OR1G1 dose–response relationships were studied with a strong elicitor (nonanal), a medium agonist (decanoic acid), and a weak agonist (1-hexanol), applying odorants at concentrations ranging from 0.01 μM to 100 μM in the 1 μl drop. As shown in Figure 2C, Ca^{2+} responses increased with odorant dose and reached a plateau at 10 μM with nonanal. While decanoic acid did not elicit a saturable response at a concentration of 100 μM, 1-hexanol elicited only a weak response even at a concentration of 100 μM.

Comparison of OR52D1 (class I) responses with OR1G1 (class II)

OR52D1/$G_{\alpha 16}$-expressing cells were tested with the same odorants as OR1G1/$G_{\alpha 16}$-expressing cells. Figure 3 shows that Ca^{2+} responses of OR52D1/$G_{\alpha 16}$-expressing cells are globally weaker than those of OR1G1/$G_{\alpha 16}$-expressing cells. The best OR52D1 Ca^{2+} response, obtained with an ester (methyl octanoate), was only in the medium range. While most alcohols induced OR1G1 responses, only some of them were able to weakly activate OR52D1. Conversely, OR52D1 Ca^{2+} responses were elicited by most of acids, while OR1G1

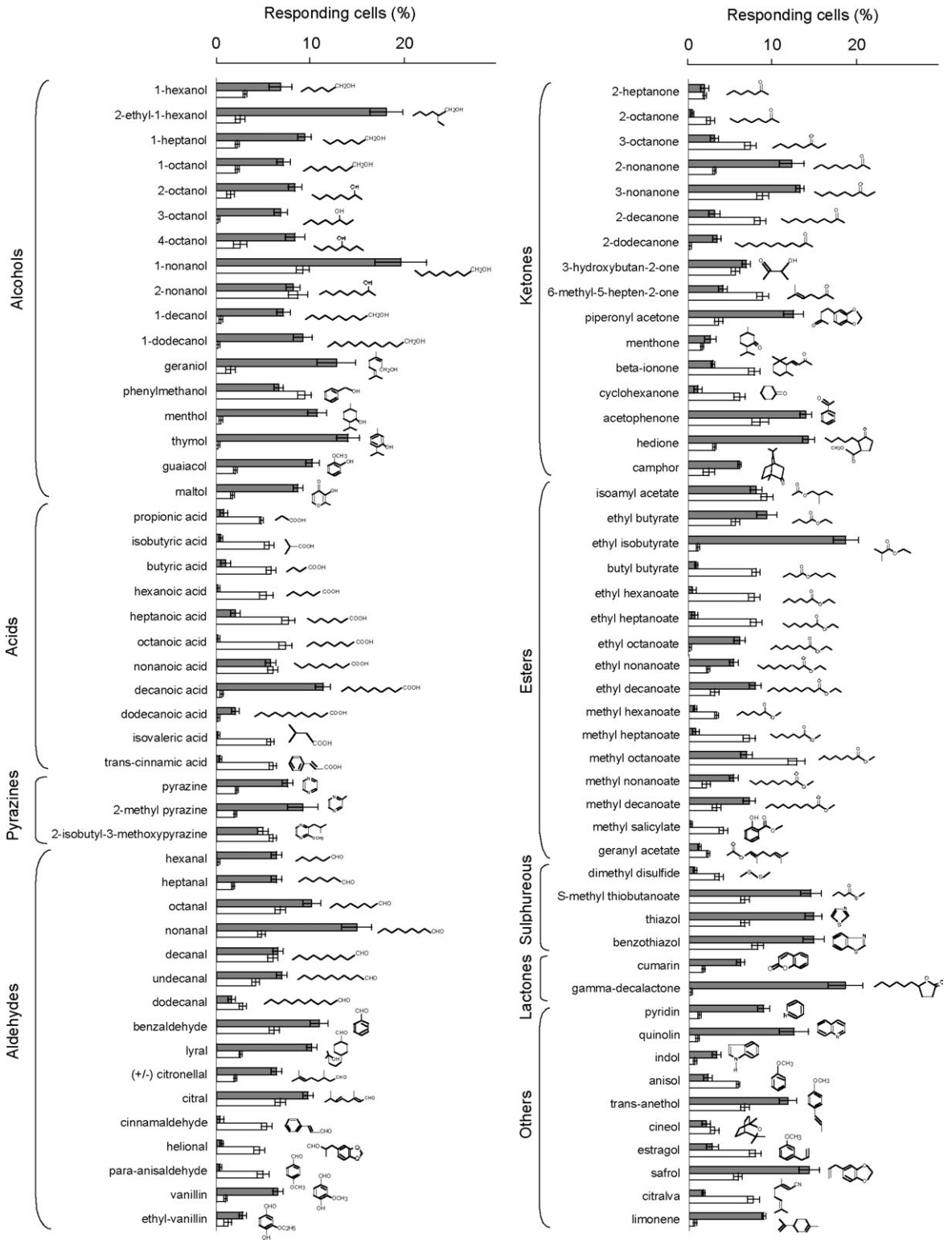

Figure 3 Comparison of OR1G1 and OR52D1 responses to various odorants using calcium imaging. HEK293 cells co-expressing OR1G1/$G_{\alpha 16}$ or OR52D1/$G_{\alpha 16}$ were stimulated using VOFA with odorants, applied as a 1 μl drop at 10 μM, which freely evaporated in the well. The data are shown as the number of responding cells normalized as a percentage of cells responding to 100 μM ATP. Greyed and open bars are used for OR1G1 and OR52D1, respectively. Bars indicate standard deviation of three independent experiments.

is only activated by two of them. In contrast to OR1G1, OR52D1 was revealed not tuned toward odorants sharing a common chain length. However, the chemical functions appeared to be important for OR52D1 activation, which is better activated by acids, aldehydes, ketones and esters than alcohols or pyrazines. The position of the functional group was not critical for OR52D1. For instance, equivalent responses were observed with ethyl heptanoate and methyl octanoate, and with 1-nonanol and 2-nonanol. Nevertheless, 3-nonanone and 3-octanone were both active whereas 2-nonanone and 2-octanone were inactive.

OR1G1 antagonists

Studying OR1G1 responses, we observed that co-applications of equimolar odorant mixtures were less active than pure odorants applied at an identical concentration. For instance, the mixture made of 1-hexanol, 1-octanol, 1-nonanol, 2-nonanol and 1-decanol elicited a weak OR1G1 Ca^{2+} response, while 1-nonanol alone was classified as a strong agonist. Similarly, the aldehyde mixture composed of hexanal, heptanal, octanal, nonanal, decanal, undecanal and dodecanal was far less active on OR1G1 than nonanal alone (strong agonist). By testing odorant couples, we found that 1-hexanol and hexanal, weak agonists by themselves, were the only OR1G1 antagonists present in alcohol and aldehyde mixtures, respectively (Figure 4A,B). We also observed that 1-nonanol-induced Ca^{2+} responses were significantly inhibited by hexanal (Figure 4A-3) and, reciprocally, nonanal-induced Ca^{2+} responses were inhibited by 1-hexanol (Figure 4B-2). Moreover, 1-hexanol and hexanal inhibited OR1G1 Ca^{2+} responses elicited by the two other strong agonists, ethyl isobutyrate and γ-decalactone (data not shown). Looking for other C6 compounds as antagonists, we tested hexanoic acid and cyclohexanone (both non-agonist molecules) against γ-decalactone as elicitor (Figure 4C). Whereas hexanoic acid had no appreciable antagonist effect (Figure 4C-2), cyclohexanone also inhibited OR1G1 γ-decalactone-induced Ca^{2+} responses (Figure 4C-3). The dose–response effect was investigated using mixtures of cyclohexanone and γ-decalactone at different ratios. Figure 4D illustrates that cyclohexanone diminished γ-decalactone-induced OR1G1 Ca^{2+} responses in a dose-dependent manner. Cyclohexanone effect was the stronger so its concentration was higher and γ-decalactone concentration lower. In order to exclude the possibility that the inhibitory effect was due to a nonspecificic effect on the transduction cascade, we stimulated the endogenous purinergic receptors of OR1G1/$G_{\alpha 16}$-expressing cells with ATP, which activates the IP3 pathway. The same Ca^{2+} responses were measured (data not shown) whether in the absence or presence of 1-hexanol and hexanal. Interestingly, methyl octanoate-induced Ca^{2+} responses of the other OR studied (OR52D1) were inhibited by neither 1-hexanol (Figure 4E) nor hexanal (data not shown), which showed that antagonist effect is OR specific.

Discussion

Human OR odorant repertoires have been described for two class II ORs (Wetzel *et al.*, 1999; Spehr *et al.*, 2003) whereas no functional data have been reported for any human class I OR. However, class I ORs have already been shown to be functional in mouse (Malnic *et al.*, 1999). Analysis of the human genome showed that class I OR genes surprisingly comprise only a few pseudogenes, suggesting that fish-like ORs assume an essential role in human olfactory sensing (Glusman *et al.*, 2001). We then compared the odorant repertoires of human ORs from both classes.

Functional analysis of the ORs was performed using the fluorescence-based assay VOFA, which involved modified HEK293 cells stimulated with odorants applied as a vapor. This simple mode of odorant delivery avoids all the problems encountered with perfused cells. However, one limitation of this odorant stimulation is the inability to know precisely the actual amount of odorant reaching the OR, impeding the determination of IC_{50} values. Morever, given the air: water partition coefficients for differents odorants applied at the same concentration in MeOH, cells were stimulated with different odorant concentrations. The odorant amount applied was minimized to clearly differentiate OR odorant responses. Odorants elicited Ca^{2+} responses at concentrations reaching the cells ranging from 10^{-8} to 10^{-6} M in a dose-dependent way. These doses are low compared with those used in most studies in which odorants were delivered by perfusion of solutions, which ranged from 10^{-6} to 10^{-3} M (Krautwurst *et al.*, 1998; Wetzel *et al.*, 1999; Gaillard *et al.*, 2002, 2004; Katada *et al.*, 2003). Stimulations with higher odorant concentrations did not improve Ca^{2+} responses, eliciting no more than 20 % of cells. This low number is probably due to inefficient $G_{\alpha 16}$-protein coupling or poor OR targeting to the plasma membrane, as already demonstrated for other ORs (Gimelbrant *et al.*, 2001; Lu *et al.*, 2004). However, Lu *et al.* (2004) have recently reported that ORs can be functionally expressed in HEK293 cells although ORs could not be visualized at the plasma membrane. They also mentioned that deltaF508 cystic fibrosis transmembrane regulator functionality was demonstrated by electrophysiological analyses while its membrane expression could not be observed. Recently, Hague *et al.* (2004) have reported that M71 OR surface expression in HEK293 cells is promoted by co-expression with β_2-adrenergic receptor (β_2-AR). As they observed for rat I7 or human OR17-40, we found that β_2-AR was unable to promote cell-surface expression of rIC6, OR1G1 and OR52D1 (data not shown).

Functional analysis of OR1G1 revealed 59 agonists. Five of them were observed to be strong, 21 medium and 33 weak, suggesting that this OR is broadly tuned toward odorants belonging to different chemical classes. Such data for a human heterologously expressed OR is in agreement with vertebrate neuron activations (Duchamp-Viret *et al.*, 1999; Malnic *et al.*, 1999; Araneda *et al.*, 2000; Ma and Shepherd,

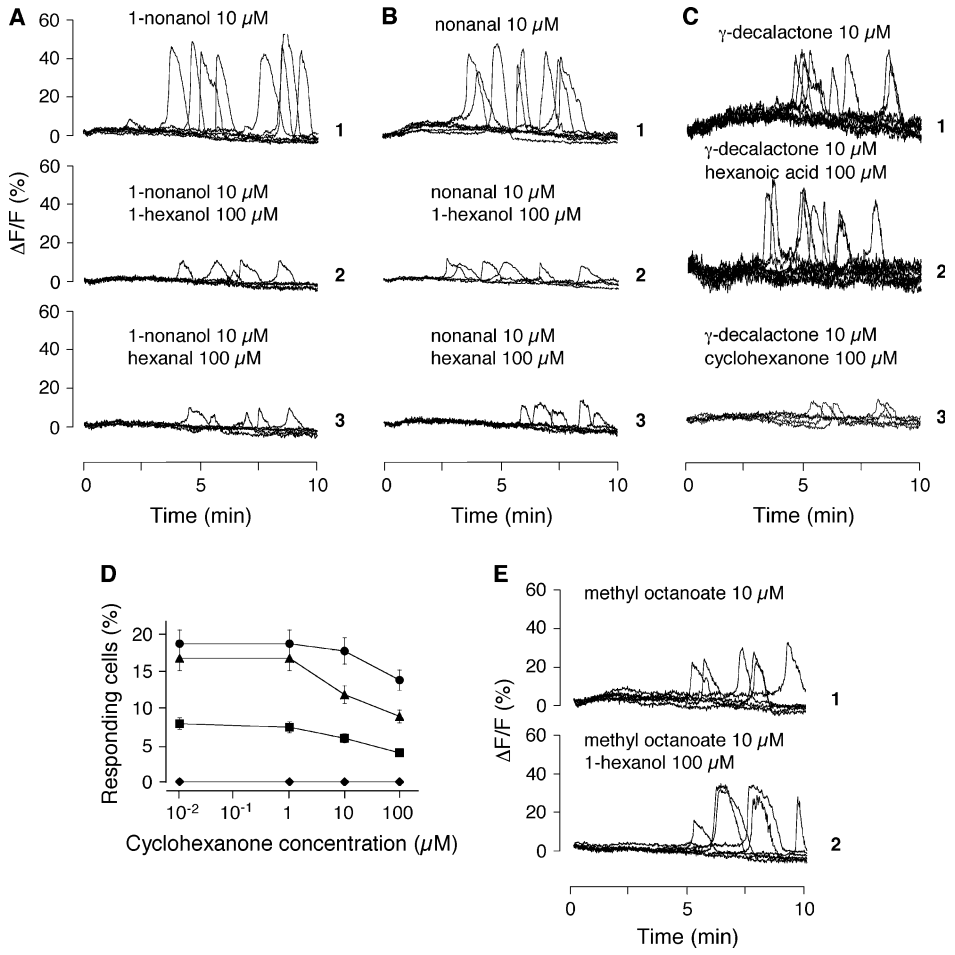

Figure 4 Antagonism of OR odorant responses. **(A)** Inhibition of 1-nonanol OR1G1 activation by 1-hexanol and hexanal. VOFA stimulation with 1-nonanol alone (1), 1-nonanol mixed with 1-hexanol (2) and 1-nonanol mixed with hexanal (3). 1-Nonanol and 1-hexanol (or hexanal) were mixed in 100% MeOH at a final concentration of 10 and 100 μM, respectively. Ca^{2+} responses were recorded during 10 min and are shown as fluorescence intensity changes (Δ*F*/*F*). **(B)** Inhibition of nonanal OR1G1 activation by 1-hexanol and hexanal. VOFA stimulation with nonanal alone (1), nonanal mixed with 1-hexanol (2) and nonanal mixed with hexanal (3). Same conditions as for (A). **(C)** Inhibition of γ-decalactone OR1G1 activation by hexanoic acid and cyclohexanone. VOFA stimulation with γ-decalactone alone (1), γ-decalactone mixed with hexanoic acid (2) and γ-decalactone mixed with cyclohexanone (3). Same conditions as for (A). **(D)** Cyclohexanone dose-dependent inhibition of OR1G1 activated by γ-decalactone. OR1G1 stimulated with cyclohexanone alone (diamonds), mixed with 1 μM (squares), 10 μM (triangles) and 100 μM (circles) γ-decalactone. γ-Decalactone and cyclohexanone were mixed in 100% MeOH and applied as a 1 μl drop using VOFA. Data are shown as the number of responding cells normalized as a percentage of the cells responding to 100 μM ATP. Bars indicate standard deviation (three independent experiments). **(E)** Effect of 1-hexanol on OR52D1 activated by methyl octanoate. VOFA stimulation with methyl octanoate alone (1) and mixed with 1-hexanol (2). Methyl octanoate and 1-hexanol were mixed in 100% MeOH at a final concentration of 10 and 100 μM, respectively. At the end of each experiment, ATP (100 μM) was applied to verify cell viability. The curves are representative Ca^{2+} responses of 5–9 responsive HEK293 cells within the same camera field.

2000), glomerular activations (Rubin and Katz, 1999; Uchida *et al.*, 2000; Leon and Johnson, 2003; Xu *et al.*, 2003) and mitral cell recordings (Mori *et al.*, 1999). Such a broad repertoire was not reported for the only class II human OR so far studied, OR17-40 (Wetzel *et al.*, 1999), and a class II human testicular OR (Spehr *et al.*, 2003) suggesting that broad tuning is not a general feature of ORs. However, it is worth noticing that these authors did not couple ORs with the IP3 pathway using an efficient promiscuous G_{α} protein, which we found to be compulsory for OR1G1 and OR52D1, as also reported for numerous rodent ORs (Krautwurst *et al.*, 1998; Touhara *et al.*, 1999; Gaillard *et al.*, 2002). Considering strong and medium OR1G1 agonists, their chemical function did not appeared to be a decisive criterium for their agonism (except acids, which were only weak activators), but their size was of prime importance, whatever aliphatic or cyclic molecules involved (Figure 5). Such an observation has been reported for neuron and glomerular activation (Kaluza and Breer, 2000; Johnson *et al.*, 2002; Xu *et al.*, 2003). The position of the functional group in aliphatic molecules was not essential for OR1G1 agonists, except 9-carbon alcohols like 1-nonanol, which was far more active than 2-nonanol. This suggests that OR1G1 binding pocket exhibits a critical size and that odorant interaction relies on hydrophobic forces within the binding site, not reinforced by amino-acid side chain interactions.

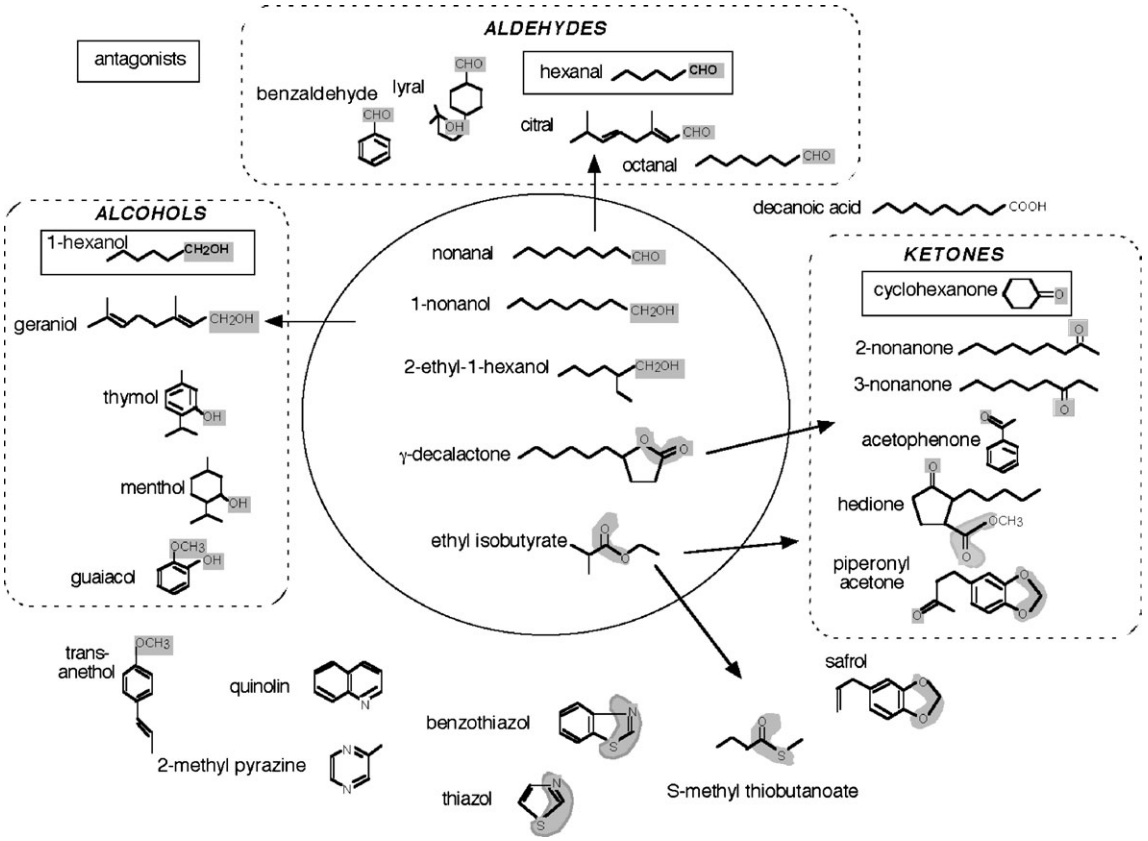

Figure 5 Structural comparison of OR1G1 ligands and antagonists. Strong agonists (>15% of responding cells) are located in the circle, while medium agonists (10–15% of responding cells) are outside and gathered by chemical classes. Antagonists are boxed. Arrows outline the chemical relationships between agonist and antagonist molecules. Peculiar structure features shared by active molecules are also highlighted in grey.

The fish-like OR52D1 receptor was observed to be functional with a more limited repertoire than the class II OR1G1. We revealed only one medium agonist (methyl octanoate) and 44 weak activators, which were globally different from OR1G1 agonists. OR52D1 activation was not as size-dependent as observed with OR1G1, suggesting a different mode of interaction with its agonists. As regards the lower odorant-induced Ca^{2+} responses of OR52D1, this receptor is either less sensitive, as already demonstrated using olfactory neurons (Araneda *et al.*, 2004), and/or less efficiently coupled to the IP3 pathway via $G_{\alpha 16}$ protein (Kostenis, 2001). One can remark that OR52D1 odorant spectrum includes the reported agonists of its murine orthologous OR (S19 sharing 65% amino-acid sequence identity), which was shown to respond to C7–C9 aliphatic acids and alcohols (Malnic *et al.*, 1999). Similarly, OR912-93 orthologs from different species (primates, pig and mouse) have been also shown to respond to common odorant molecules (2- and 3-heptanone) (Gaillard *et al.*, 2004). Moreover, phylogenetic comparison of human and mouse OR genes has revealed a very similar overall distribution of ORs, suggesting that they may cover a close receptor space (Zhang and Firestein, 2002). Our observation that orthologous ORs between humans and rodents have similar agonist repertoire supports this hypothesis.

While well documented in other G-protein coupled receptors, antagonists at a receptor level were recently reported for rodent ORs (Araneda *et al.*, 2000; Duchamp-Viret *et al.*, 2003; Oka *et al.*, 2004) as well as for human spermatozoa ORs (Spehr *et al.*, 2003). Here, we found odorants that diminish the odorant-induced Ca^{2+} response of a human class II OR in a dose-dependent manner. The occurrence of such odorant antagonists in a mixture hampers the observation of activators, which casts doubt on studies of OR repertoires using odorant mixtures (Wetzel *et al.*, 1999; Gaillard *et al.*, 2002). The identified OR1G1 antagonists were all 6-carbon molecules (Figure 5), observed to be either weak agonists (1-hexanol, hexanal) or a non-agonist molecule (cyclohexanone). Antagonists share a functional group with strong (alcohol, aldehyde) and medium (ketone) agonists. Thus, cyclohexanone is close to benzaldehyde and other cyclic molecules that induce OR1G1 responses. Reciprocally, hexanoic acid was not an antagonist, just like aliphatic acids were not strong agonists. The occurrence of common features between agonists and antagonists has already been reported (Spehr *et al.*, 2003; Araneda *et al.*, 2004; Oka *et al.*, 2004) and suggests that odorant antagonists act as competitive inhibitors for the binding pocket. Such a hypothesis is supported by the quantitative variation of OR1G1 inhibition at

different agonist and antagonist ratios (Figure 4D). Nevertheless, the determination of IC_{50} values, critical for distinguishing between competitive and allosteric mechanisms, was not possible using VOFA. On a structural point of view, since 6-carbon antagonists share functional groups with 9-carbon agonists, one can speculate that they bind the OR1G1 odorant pocket at its entry, making interactions through their chemical function at the entrance of the binding site. Likely due to a too short chain length, they would not reach the bottom of the active site, which would be involved in OR signal transduction triggering. A similar hypothesis could account for differences in OR1G1 activation by odorants distinguished by the position of their functional group on the aliphatic chain (1-nonanol and 2-nonanol, for instance). This is also in agreement with the observation that OR1G1 antagonists did not affect agonist-induced Ca^{2+} responses of OR52D1, which suggests that antagonists are receptor specific. Similarly, undecanal, the antagonist of the human testicular receptor OR17-4 (Spehr *et al.*, 2003) was unable to inhibit OR1G1 Ca^{2+} response. These observations support the hypothesis that olfactory sensing results from combinatorial coding of both agonists and antagonists at OR level (Oka *et al.*, 2004), which may explain changes in perception of odours in a mixture.

In conclusion, the odorant repertoire of two human ORs, one belonging to class I (fish-like) and the other to class II (terrestrial-type), established with 100 odorants applied in their vapor phase, delineated that (i) for the first time, a human class I OR was observed to be functional with a narrow repertoire related to that of its mouse ortholog; (ii) the class II OR is broadly tuned toward molecules of 9 or 10 carbons, with diverse functional groups; and (iii) antagonists against this latter OR shared common features with agonists but with a shorter 6-carbon chain length, with a dose-dependent antagonist effect. Molecular modeling and docking would direct mutagenesis in order to decipher the 3-D structure of the binding site, allowing elucidation of the structure–activity relationships of these human ORs. Such an approach might help understanding how odorant inhibition occurs at the first level of sensory detection, which seems to be a general feature that may be involved in odor masking.

Acknowledgements

We thank P. Adenot for use of the INRA confocal facility.

References

Abdulaev, N.G., Popp, M.P., Smith, W.C. and **Ridge, K.D.** (1997) *Functional expression of bovine opsin in the methylotrophic yeast* Pichia pastoris. Protein Expr. Purif., 10, 61–69.

Araneda, R.C., Kini, D. and **Firestein, S.** (2000) *The molecular receptive range of an odorant receptor.* Nat. Neurosci., 3, 1248–1255.

Araneda, R.C., Peterlin, Z., Zhang, X., Chesler, A. and **Firestein, S.** (2004) *A pharmacological profile of the aldehyde receptor repertoire in rat olfactory epithelium*. J. Physiol., 555, 743–756.

Buettner, J.A., Glusman, G., Ben-Arie, N., Ramos, P., Lancet, D. and **Evans, G.A.** (1998) *Organization and evolution of olfactory receptor genes on human chromosome 11*. Genomics, 53, 56–68.

Bulger, M., van Doorninck, J.H., Saitoh, N., Telling, A., Farrell, C., Bender, M.A., Felsenfeld, G., Axel, R., Groudine, M. and **von Doorninck, J.H.** (1999) *Conservation of sequence and structure flanking the mouse and human beta-globin loci: the beta-globin genes are embedded within an array of odorant receptor genes*. Proc. Natl Acad. Sci. USA, 96, 5129–5134.

Cometto-Muniz, J.E., Cain, W.S., Abraham, M.H. and **Gola, J.M.** (1999) *Chemosensory detectability of 1-butanol and 2-heptanone singly and in binary mixtures*. Physiol. Behav., 67, 269–276.

Duchamp-Viret, P., Chaput, M.A. and **Duchamp, A.** (1999) *Odor response properties of rat olfactory receptor neuron*. Science, 284, 2171–2174.

Duchamp-Viret, P., Duchamp, A. and **Chaput, M.A.** (2003) *Single olfactory sensory neurons simultaneously integrate the components of an odour mixture*. Eur. J. Neurosci., 18, 2690–2696.

Freitag, J., Krieger, J., Strotmann, J. and **Breer, H.** (1995) *Two classes of olfactory receptors in Xenopus laevis*. Neuron, 15, 1383–1392.

Gaillard, I., Rouquier, S., Pin, J.P., Mollard, P., Richard, S., Barnabé, C., Demaille, J. and **Giorgi, D.** (2002) *A single olfactory receptor specifically binds a set of odorant molecules*. Eur. J. Neurosci., 15, 409–418.

Gaillard, I., Rouquier, S., Chavanieu, A., Mollard, P. and **Giorgi, D.** (2004) *Amino-acid changes acquired during evolution by olfactory receptor 912–93 modify the specificity of odorant recognition*. Hum. Mol. Genet., 13, 771–780.

Gimelbrant, A.A., Haley, S.L. and **McClintock, T.S.** (2001) *Olfactory receptor trafficking involves conserved regulatory steps*. J. Biol. Chem., 276, 7285–7290.

Glusman, G., Yanai, I., Rubin, I. and **Lancet, D.** (2001) *The complete human olfactory subgenome*. Genome Res., 11, 685–702.

Hague, C., Uberti, M., Chen, Z., Bush, C.F., Jones, S.V., Ressler, K.J., Hall, R.A. and **Minneman, K.P.** (2004) *Olfactory receptor surface expression is driven by association with the β_2-adrenergic receptor.* Proc. Natl Acad. Sci. USA, 101, 13672–13676.

Johnson, B.A., Ho, S.L., Xu, Z., Yihan, J.S., Yip, S., Hingco, E.E. and **Leon, M.** (2002) *Functional mapping of the rat olfactory bulb using diverse odorants reveals modular responses to functional groups and hydrocarbon structural features*. J. Comp. Neurol., 449, 180–194.

Kajiya, K., Inaki, K., Tanaka, M., Haga, T., Kataoka, H. and **Touhara, K.** (2001) *Molecular bases of odor discrimination: reconstitution of olfactory receptors that recognize overlapping sets of odorants*. J. Neurosci., 21, 6018–6025.

Kaluza, J.F. and **Breer, H.** (2000) *Responsiveness of olfactory neurons to distinct aliphatic aldehydes*. J. Exp. Biol., 203, 927–33.

Katada, S., Nakagawa, T., Kataoka, H. and **Touhara, K.** (2003) *Odorant response assays for a heterologously expressed receptor.* Biochem. Biophys. Res. Commun., 305, 964–969.

Kostenis, E. (2001) *Is Galpha16 the optimal tool for fishing ligands of orphan G-protein-coupled receptors?* Trends Pharmacol. Sci., 22, 560–564.

Krautwurst, D., Yau, K.W. and **Reed, R.R.** (1998) *Identification of ligands for olfactory receptors by functional expression of a receptor library.* Cell, 95, 917–926.

Laing, D.G. and **Francis, G.W.** (1989) *The capacity of humans to identify odors in mixtures*. Physiol. Behav., 46, 809–814.

Leon, M. and **Johnson, B.A.** (2003) *Olfactory coding in the mammalian olfactory bulb*. Brain Res. Rev., 42, 23–32.

Li, X., Staszewski, L., Xu, H., Durick, K., Zoller, M. and **Adler, E.** (2002) *Human receptors for sweet and umami taste*. Proc. Natl Acad. Sci. USA, 99, 4692–4696.

Lu, M., Staszewski, L., Echeverri, F., Xu, H. and **Moyer, B.D.** (2004) *Endoplasmic reticulum degradation impedes olfactory G-protein coupled receptor functional expression.* BMC Cell Biol., 5, 34.

Ma, M. and **Shepherd, G.M.** (2000) *Functional mosaic organization of mouse olfactory receptor neurons*. Proc. Natl Acad. Sci. USA, 97, 12869–12874.

Malnic, B., Hirono, J., Sato, T. and **Buck, L.B.** (1999) *Combinatorial codes for odors*. Cell, 96, 713–723.

Malnic, B., Godfrey, P.A. and **Buck L.B.** (2004) *The human olfactory receptor gene family.* Proc. Natl Acad. Sci. USA, 101, 2584–2589.

Matarazzo, V., Zsurger, N., Guillemot, J.C., Clot-Faybesse, O., Botto, J.M., Dal Farra, C., Crowe, M., Demaille, J., Vincent, J.P., Mazella, J. and **Ronin, C.** (2002) *Porcine odorant-binding protein selectively binds to a human olfactory receptor.* Chem. Senses, 27, 691–701.

Mori, K., Nagao, H. and **Yoshihara, Y.** (1999) *The olfactory bulb: coding and processing of odor molecule information*. Science, 286, 711–715.

Ngai, J., Dowling, M.M., Buck, L., Axel, R. and **Chess, A.** (1993) *The family of genes encoding odorant receptors in the channel catfish*. Cell, 72, 657–666.

Oka, Y., Omura, M., Kataoka, H. and **Touhara, K.** (2004) *Olfactory receptor antagonism between odorants.* EMBO J., 23, 120–126.

Rubin, B.D. and **Katz, L.C.** (1999) *Optical imaging of odorant representations in the mammalian olfactory bulb*. Neuron, 23, 499–511.

Spehr, M., Gisselmann, G., Poplawski, A., Riffel, J.A., Wetzel, C.H., Zimmer, R.K. and **Hatt, H.** (2003) *Identification of a testicular odorant receptor mediating human sperm chemotaxis*. Science, 299, 2054–2058.

Touhara, K., Sengoku, S., Inaki, K., Tsuboi, A., Hirono, J., Sato, T., Sakano, H. and **Haga, T.** (1999) *Functional identification and reconstitution of an odorant receptor in single olfactory neurons*. Proc. Natl Acad. Sci. USA, 96, 4040–4045.

Uchida, N., Takahashi, Y.K., Tanifuji, M. and **Mori, K.** (2000) *Odor maps in the mammalian olfactory bulb: domain organization and odorant structural features*. Nat. Neurosci., 3, 1035–1043.

Wetzel, C.H., Oles, M., Wellerdieck, C., Kuczkowiak, M., Gisselmann, G. and **Hatt, H.** (1999) *Specificity and sensitivity of a human olfactory receptor functionally expressed in human embryonic kidney 293 cells and* Xenopus Laevis *oocytes*. J. Neurosci., 19, 7426–7433.

Xu, F., Liu, N., Kida, I., Rothman, D.L., Hyder, F. and **Shepherd, G.M.** (2003) *Odor maps of aldehydes and esters revealed by functional MRI in the glomerular layer of the mouse olfactory bulb*. Proc. Natl Acad. Sci. USA, 100, 11029–11034.

Zhang, X. and **Firestein, S.** (2002) *The olfactory receptor gene superfamily of the mouse*. Nat. Neurosci., 5, 124–133.

Zozulya, S., Echeverri, F. and **Nguyen, T.** (2001) *The human olfactory receptor repertoire.* Genome Biol., 2, RESEARCH0018.

Accepted November 8, 2004